Title

Anti-non-Gal-specific combination treatment with an anti-idiotypic Ab and an inhibitory small molecule mitigates the xenoantibody response

Journal

Xenotransplantation, 21(3)

ISSN

0908-665X

Authors

Stewart, John M
Tarantal, Alice F
Chen, Yan
et al.

Publication Date

2014-05-01

DOI

10.1111/xen.12096

Peer reviewed

Published in final edited form as:
Xenotransplantation. 2014 May ; 21(3): 254–266. doi:10.1111/xen.12096.

Anti-nonGal specific combination treatment with an anti-idiotypic Ab and an inhibitory small molecule mitigates the xenoantibody response

John M. Stewart[1], **Alice F. Tarantal**[2], **Yan Chen**[1], **Nancy Appleby**[1], **Tania Fuentes**[1], **C. Chang I. Lee**[2], **Evelyn J. Salvaris**[3], **Anthony J.F. d'Apice**[3], **Peter J. Cowan**[3], and **Mary Kearns-Jonker**[1]

Mary Kearns-Jonker: mkearnsjonker@llu.edu

[1]Department of Human Anatomy, Loma Linda University School of Medicine, Loma Linda, CA

[2]Departments of Pediatrics and Cell Biology and Human Anatomy, and California National Primate Research Center, University of California, Davis, CA, USA

[3]Immunology Research Centre, St. Vincent's Hospital Melbourne, and Department of Medicine, University of Melbourne, Victoria, Australia

Abstract

Background—B cell depletion significantly extends survival of α-1,3-galactosyltranferase knockout (GTKO) porcine organs in pig-to-primate models. Our previous work demonstrated that the anti-nonGal xenoantibody response is structurally restricted. Selective inhibition of xenoantigen-xenoantibody interactions could prolong xenograft survival while preserving B cell-mediated immune surveillance.

Methods—The anti-idiotypic antibody, B4N190, was selected from a synthetic human phage display library after enrichment against a recombinant anti-nonGal xenoantibody followed by functional testing *in vitro*. The inhibitory small molecule, JMS022, was selected from the NCI diversity set III using virtual screening based on predicted xenoantibody structure. Three rhesus monkeys were pretreated with anti-nonGal specific single chain anti-idiotypic antibody, B4N190. A total of five monkeys, including two untreated controls, were then immunized with GTKO porcine endothelial cells to initiate an anti-non α-1,3-gal (nonGal) xenoantibody response. The efficacy of the inhibitory small molecule specific for anti-nonGal xenoantibody, JMS022, was tested *in vitro*.

Results—After the combination of *in vivo* anti-id and *in vitro* small molecule treatments, IgM xenoantibody binding to GTKO cells was reduced to pre-immunization levels in 2/3 animals, however, some xenoantibodies remained in the third animal. Furthermore, when treated with anti-id alone all three experimental animals displayed a lower anti-nonGal IgG xenoantibody response compared to controls. Treatment with anti-idiotypic antibody alone reduced IgM xenoantibody response intensity in only one of three monkeys injected with GTKO pig endothelial cells. In the one experimental animal which displayed reduced IgM and IgG responses select B cell subsets

Address for Correspondence: Mary Kearns-Jonker, Loma Linda University / Division of Human Anatomy, 24760 Stewart St. Ste 2215, Loma Linda, CA 92350, Tel +1 909 558 8694.

were also reduced by anti-id therapy alone. Furthermore, natural antibody responses, including anti-laminin, anti-ssDNA, and anti-throglobulin antibodies were intact despite targeted depletion of anti-nonGal xenoantibodies *in vivo* indicating that selective reduction of xenoantibodies can be accomplished without total B cell depletion.

Conclusions—This preliminary study demonstrates the strength of approaches designed to selectively inhibit anti-nonGal xenoantibody. Both anti-nonGal specific xenoantibody and small molecules can be used to selectively limit xenoantibody responses.

Keywords

Xenotransplantation; anti-idiotypic antibody; small molecule; B cell; natural antibody; phage display library

Introduction

Hyperacute rejection of porcine organs in pig-to-primate models has been circumvented by the production of α-1,3-galactosyltransferase knockout (GTKO) pigs, anti-gal antibody depleting reagents, and α-1,3-gal molecular chimerism (1-5). However, overcoming the delayed immune response induced by transplantation of porcine xenografts, genetically modified or otherwise, has been an ongoing challenge (6-10). Non α-1,3-gal (nonGal) immunogens present on porcine cells induce delayed humoral xenograft rejection (DHXR). Further transgenic modification to regulate complement and hemostasis still fails to prevent DHXR, suggesting that additional approaches are necessary to control xenoantibody responses.

The impact of the humoral immune response on xenotransplantation is illustrated by the survival of cardiac xenografts up to 8 months after the addition of B cell depleting (anti-CD20) therapy to the immunosuppressive regimen (11). However, in human allotransplantation, anti-CD20, in combination with typical immunosuppressive regimens, results in a greater risk of infection-related death (12). Due to the requirement for higher levels of immunosuppression in xenotransplantation, anti-CD20 therapy represents a greater risk for infection-related mortality. Nevertheless, B cells represent a major hurdle to successful clinical xenotransplantation in spite of their role as an essential component of the adaptive immune response.

Targeted inhibitors of anti-nonGal xenoantibodies in place of anti-CD20 therapy should mitigate DHXR while preserving overall B cell-mediated immune surveillance. Our group has demonstrated that anti-nonGal xenoantibody responses in multiple pig-to-primate models are structurally restricted (13, 14), suggesting the feasibility of selectively inhibiting the initiating nonGal antigen-xenoantibody interactions and the resulting immune response. In the current study, we report the efficacy of combination therapy using a novel single chain anti-idiotypic monoclonal antibody (mAb) and a small molecule inhibitor on the xenoantibody response to GTKO cells. These reagents were independently selected for specific reactivity to a restricted group of anti-nonGal xenoantibodies, providing a targeted approach to inhibiting the induction of xenoantibody responses against GTKO pig cells.

Materials and Methods

Animals

Five juvenile (11-12 months; 2.1-2.4 Kg) rhesus macaques (*Macaca mulatta*) from the California National Primate Research Center, University of California, Davis, CA were housed in accordance with established protocols and all procedures were in accordance with the requirements of the Animal Welfare Act. Protocols were approved prior to implementation by the University of California, Davis Institutional Animal Care and Use Committee.

Generation of Recombinant Anti-nonGal Single Chain Xenoantibody

We have recently reported the isolation and cloning of IgM cDNA sequences from baboons actively responding to genetically modified GTKO/hCD55/hCD59/hHT multiple transgenic donors (14). The IgHV3-66 and IgKV1D-12 genes encoding anti-nonGal xenoantibodies elicited by porcine islet cells in this model were inserted into the pHEN2 vector [Center for Protein Engineering, Medical Research Council Center (MRC) Cambridge, UK] (15) to generate a monoclonal, recombinant single chain anti-nonGal xenoantibody construct, H66K12. The primers used to clone the IGHV gene were LD3 and VH3BackSFI for the first reaction and JH4XHOI and VH3BackSFI for the second reaction. The light chain primers were ApaL1.K1D12 and IGJK12NotI. All reactions included 30 cycles; each cycle was 94°C for 30 seconds, 51°C for 30 seconds, and 72°C for 1 minute. The construct was inserted in frame as determined by sequencing (Beckman Research Institute at the City of Hope, Duarte, CA) using pHEN-SEQ and For_LinkSeq primers. Primer sequences were as follows: LD3 5′ TCT GGG GGA GGC TTG GTC 3′; VH3BackSFI 5′ GTC CTC GCA ACT GCG GCC CAG CCG GCC ATG GCC CAG GTG CAG CTG GTT GAG TCT GGT CG 3′; JH4XHOI 5′ TCG ACC TCG AGC TGA GGA GAC GGT GAC CAG GAC TCC CTG GCC CCA GTA GTC CAC CAC TAT AGT AAA AAC ACC CCC TCT CGC 3′; ApaL1.K1D12 5′ GTC CTC GCA ACT GCG TGC ACA GGA CAT CCA GAT GAC CCA GTC TCC ATC TTC CGT GTC TGC ATC TGT AGG AGA CAA AGT C 3′; IGJK12NotI 5′ TCG ACG CGG CCG CTT TGA TCT CCA CTT TGG TCC CCT GGC CAA AAC TGT ACG GGT AAC TAC TAC CCT GTC GAC AGT AAT AA 3′; pHEN-SEQ 5′ CTA TGC GGC CCC ATT CA 3′; FOR_LinkSeq 5′ GCC TTT TCT GTA TGA GG 3′

Expression and Purification of Single Chain Antibody

Chemically competent *E. coli* strain HB2151 were transformed with the single chain pHEN2 DNA construct. Bacterial overnight growth was used at a 1:100 dilution to seed fresh 2×TY media (1% glucose, 1% Ampicillin). Freshly diluted bacteria were grown shaking at 37°C and 225 rpm until the optical density at 600 nm was 0.8-0.9. Isopropyl β-D-1-thiogalactopyranoside was added to a final concentration of 1 mM and left to incubate for 20-24 hours shaking at 225 rpm and 30°C. Bacteria were cleared by centrifugation at 1,800 g at 4°C.

Protein in the bacterial supernatant was concentrated by ammonium sulfate precipitation at 80% saturation (0°C). Precipitated protein was pelleted by centrifugation for 15 minutes, 10,000 g at 4°C, then resuspended to 1/50 initial volume in cold PBS. Concentrated protein

was then dialyzed at 4°C overnight against PBS to remove remaining ammonium sulfate. Protein was subsequently purified using Ni-NTA agarose resin according to manufacturer instructions (Qiagen, Carlsbad, CA) except for the use of 10 mM imidazole in washing and preparation of binding solutions. Protein was subjected to Ni-NTA chromatography a second time to ensure purity. Flow through, washes, and elutions were saved for analysis by sodium dodecylsulphate polyacrylamide gel electrophoresis and visualized using either silver stain (Thermo Scientific, Rockford, IL) or Imperial Protein Stain (Thermo Scientific). Purified single chain variable fragment (scFv) concentration was determined using a standard curve of carbonic anhydrase (Sigma, St. Louis, MO) and quantifying protein staining using Image J software (16).

Enrichment of H66K12-Reactive Single Chain Antibody

Nunc Maxisorp Immunotubes (Fisher, Chino, CA) were coated overnight with purified H66K12 single chain mAb (10-50 μg/ml). The Griffin.1 phagemid library (17) was incubated in the coated immunotubes at 37°C for two hours. After PBST wash, remaining phage particles were used to infect an exponentially growing culture of the *E. coli* strain TG1. Before subsequent rounds of selection, polyclonal phagemid was prepared by infecting TG1 with M13K07 helper phage (Life Technologies, Carlsbad, CA) at a ratio of 1:20 (bacteria: helper phage) incubating at 30°C shaking overnight. Bacteria were cleared by centrifugation at 1,800 g for 10 minutes and supernatant saved for further rounds of selection. The enrichment process was repeated a total of 5 times, however sequencing for full length constructs in frame without premature amber stop codons was performed starting after the third enrichment. Overall enrichment after each selection was assessed by ELISA against purified H66K12 using scFv expressed on the surface of filamentous phage. Constructs encoding full length scFv were identified by PCR using the LMB3 and pHENseq primers. The reaction included 31 cycles; each cycle was 94°C for 30 seconds, 55°C for 60 seconds, and 72°C for 30 seconds.

Preparation of Monoclonal Antibody

Polyclonal phagemid preparations were used to infect TG1. Infected TG1 were subsequently plated on TYE plates (1% ampicillin). Single colonies were considered to be monoclonal. Phage was prepared by infecting TG1 with M13K07 helper phage (Life Technologies, Carlsbad, CA) at a ratio of 1:20 (bacteria: helper phage) incubating at 30°C shaking overnight. Bacteria were cleared by centrifugation at 1,800 g for 10 minutes. Soluble scFv was prepared by transforming HB2151 with pHEN2 DNA extracted from bacterial overnight preparations using the QIAprep Spin Miniprep Kit (Qiagen, Carlsbad, CA). PCR of pHEN2 DNA using the LMB3 and pHEN_seq primers was used to screen for full length single chain constructs. PCR conditions were 25 cycles; each cycle was 94°C for 30 seconds, 49°C for 30 seconds, and 72°C for 30 seconds. LMB3 5′ ACA GGA AAC AGC TAT GAC 3′

Xenotransplantation

All animals were prescreened for low levels of nonGal-reactive xenoantibody by ELISA using GTKO endothelial cells (PEGKO42) which were kindly provided by Dr. David Sachs,

Massachusetts General Hospital. The experimental time line is illustrated in Figure 1. Blood draws for serum and B cell analysis were taken at each experimental time point. Two control animals were intravenously injected with 60×10^6 GTKO endothelial cells. This infusion model elicits a xenoantibody response without the procedural complications of solid organ transplantation. Three experimental animals were intravenously injected with 200-250 μg of anti-idiotypic antibody once per week for three weeks before immunization with GTKO endothelial cells. We hypothesized that by immunizing with fewer cells, we would see a reduced xenoantibody response and, potentially, a greater effect of pretreatment with anti-idiotypic antibody. Thus, experimental animals were injected with either 60×10^6, 15×10^6, or 7.5×10^6 GTKO porcine endothelial cells, respectively.

Molecular Modeling and Screening of Small Molecules

All protein modeling was performed using the Discovery Studio 3.5 suite (Accelrys, San Diego, CA). Representative amino acid sequences were derived from cloned heavy and light chain cDNA sequences of IgM xenoantibodies induced in baboons at 28 days after transplantation of GTKO/hCD55/hCD59/hHT transgenic porcine islets (14). The variable domain model of H66K12 was prepared by homology modeling using a Modeller algorithm optimized for antibody modeling. Structural refinement of the heavy chain CDR3 was performed using the loop refinement protocol. Autodock vina (18) in combination with PyRx (19) were used to locally perform virtual screening of the Diversity Set III of small molecules provided by the NCI/DTP Open Chemical Repository (http://dtp.cancer.gov).

Flow Cytometry

A total of 50 μL of whole blood was stained with CD10 mAb (clone HI10a-PE; BD Biosciences, San Jose, CA), CD20 (clone 2H7-PerCP; BD Biosciences), CD21 (clone B-ly4-APC; BD Biosciences), and CD27 (clone M-T271-FITC; BD Biosciences) for 20 minutes at room temperature. Red blood cells were lysed using the Coulter Q-Prep (Beckman Coulter, Fullerton, CA). A FACSCalibur flow cytometry system (BD Biosciences) was used for these studies. Isotype control IgG was used as a negative control (BD Biosciences). Mononuclear cells were gated by their forward- and side-scatter characteristics to exclude contaminating red blood cells, granulocytes, and monocytes. A minimum of 1×10^4 cells were analyzed for each sample with CellQuest software. The absolute number of PBMCs analyzed at each time point is indicated in Table 1.

Screening for reactivity of the anti-idiotypic antibodies *in vitro* by flow cytometry

Post xenotransplant serum (1:100) with or without single chain antibody (80 μg/ml) was incubated with GTKO porcine endothelial cells for 1 hour at room temperature. Monkey IgM bound to GTKO endothelial cells was labeled using FITC conjugated Goat anti-human IgM (1:100) (Jackson Immunoresearch, West Grove, PA). Data was acquired with a MACSQuant flow cytometer (Becton Dickinson, San Diego, CA) and analyzed with FlowJo software (Tree stars, Ashland, OR).

ELISA

The xenoantibody response was measured by ELISA using GTKO endothelial cells as targets, as previously described (20). Serum pre and post-transplant was diluted (1:30) in blocking buffer in the presence or absence of small molecules at a concentration of 30 μg/ml to test for inhibition of induced antibody responses to GTKO cells. Calf thymus single stranded DNA (ssDNA) (Sigma, St. Louis, MO), mouse laminin (Sigma, St. Louis, MO), and human thyroglobulin (Scipac, Sittingbourne, Kent, UK) were precoated on the 96 well plates at a concentration of 20 μg/well. Xenoantibody serum was incubated on the coated plates for one hour at room temperature prior to incubation with secondary antibodies. Anti-human IgM HRP (1:5000) (Jackson Immunoresearch, West Grove, PA), human IgG HRP (1:1000) (Sigma), and anti-M13 HRP (1:500) (GE-Healthcare, Buckinghamshire, UK) were used as secondary antibodies for the ELISAs performed in this study. Rhesus monkey serum used in control experiments for natural antibody levels came from seven age-matched monkeys prescreened for relatively low levels of anti-nonGal IgM and IgG xenoantibody as determined by ELISA. Samples were repeated in triplicate, ELISAs were repeated at least twice.

Statistical analysis

All statistical analyses were performed using Excel. When error bars are present, data is represented as mean ± standard error of the mean (SEM) of three technical replicates unless indicated otherwise. Statistical significance (p-value < 0.05) compared to the untreated control was established using a Student's t-test.

Results

Generation of Anti-idiotypic Single Chain Antibodies

After three rounds of enrichment using purified H66K12 a dramatic increase in the total binding of the polyclonal phagemid pool to the xenoantibody target was noted (Figure 2a). However, an additional two rounds of enrichment and screening was necessary to increase the yield of full length constructs without premature amber stop codons; a problem which frequently plagues phage display technology (21). Monoclonal antibody constructs were isolated from overnight growth of single colonies obtained by streaking the polyclonal pool of transformed TG1 *E. coli* on fresh TYE plates containing ampicillin. Over 1152 constructs were screened in total. Only 123 of these were approximately full length as determined by PCR (Figure 2b). Eight of these were in frame while only two did not contain premature amber stop codons. These constructs were used to transform HB2151 E. coli, expressed as scFv, purified, and assayed for their ability to inhibit induced anti-nonGal IgM xenoantibody binding to GTKO porcine endothelial cells *in vitro*, as assessed by flow cytometry. Notably, one construct, B4N190, was able to inhibit 55 ± 7% of total binding that was induced after transplantation of monkeys with GTKO cells. This anti-idiotypic antibody, encoded by the IGHV2-70 and IGLV4-3 germline genes (Figure 2c-e), was chosen for *in vivo* experimentation.

Induction Therapy with Anti-Idiotypic Antibody is Associated with a Reduction of the anti-nonGal Xenoantibody Response

We reasoned that the B cell response of animals with low levels of preexisting anti-nonGal xenoantibody would be easier to control by pretreating with anti-idiotypic antibody; as preexisting soluble anti-nonGal IgM would compete for anti-idiotypic antibody with membrane bound anti-nonGal IgM and antagonize inhibition of B cell activation. Thus, all animals were prescreened for low levels of nonGal-reactive xenoantibody by ELISA against GTKO endothelial cells. Of sixteen candidate animals, one demonstrated dramatically higher (2 fold over average) levels of anti-nonGal IgM antibodies when compared to the other monkeys. The remaining fifteen animals demonstrated moderate to low anti-nonGal xenoantibody levels (0.0-1.5 fold over background). Within this group, the animals with the lowest pre-existing anti-nonGal antibody levels (0.0-0.8 fold over background) were selected for experimentation.

The experimental time line is illustrated in Figure 1. Control monkeys were each immunized with GTKO porcine endothelial cells to stimulate an anti-nonGal xenoantibody response. Experimental monkeys each received one injection of the anti-idiotypic antibody B4N190 per week for three weeks before immunization with GTKO porcine endothelial cells at experimental day 28. Experimental animals Mo-E.A-Mo-E.C were immunized with 60×10^6, 15×10^6, and 7.5×10^6 cells, respectively. We hypothesized that by immunizing with fewer cells, we would see a reduced xenoantibody response and, potentially, a greater effect of pretreatment with anti-idiotypic antibody.

The experimental monkeys receiving induction therapy with anti-idiotypic antibody maintained low levels of nonGal IgM xenoantibodies prior to exposure to xenoantigens (Figure 3). The anti-nonGal xenoantibody antibody levels at day 0 and 14 after immunization were compared in each animal (Figure 4). The IgG but not IgM responses of experimental animals varied according the number of cells used for the immunization. After induction therapy, immunization with 60×10^6 GTKO cells did not induce a significant anti-nonGal IgM xenoantibody response (Figure 4a-b, Mo-E.A). Anti-nonGal IgM xenoantibodies were induced in the remaining two animals despite the fact that they were immunized with fewer cells. Importantly, pretreatment with B4N190 significantly reduced the IgG xenoantibody responses of all three animals (Figure 4c-d).

Reduction of Specific B cell Subsets is Associated with Low Anti-nonGal Xenoantibody Responses

B cell subsets were monitored each week to determine whether single chain anti-idiotypic antibody generated against recombinant anti-nonGal IgM xenoantibody would reduce the numbers within specific subsets of the B cell population. Induction therapy in the most responsive animal Mo-E.A, was associated with a steady reduction of immature B cells ($CD10^+/CD20^-$) (Figure 5a), total $CD20^+$ B cells (Figure 5b), and mature B cells (Figure 5c). While naïve B cells were not specifically monitored, they likely shared this trend as $CD20^+/CD21^-$ B cells (naïve/memory) but not memory B cells (Figure 5e) progressively declined. As expected, differentiated B cell ($CD20^-/CD27^+$) count prior to immunization was not affected by anti-idiotypic antibody (Figure 5f); as differentiated B cells produce

soluble but not membrane bound antibody. However, all control animals displayed an increase in cell count after immunization while those treated with B4N190 did not (Figure 6). As expected, induction therapy appears to directly impact the maturation of new differentiated B cells.

Natural Antibodies are Not Affected by Induction Therapy with B4N190

B4N190 was developed to specifically inhibit anti-nonGal xenoantibody. Because Mo-E.A is the only monkey that displayed a clear reduction of both the anti-nonGal IgM and IgG xenoantibody responses, we sought to determine if other antibody responses of this animal were still left intact. The steady levels of memory B cells in peripheral blood suggested B4N190 would not alter secondary responses against non-xenoantigens. Because B4N190 induction therapy is associated with diminishing early and mature B cells, we sought to determine whether B4N190 would alter the natural antibody response to ssDNA, thyroglobulin, and laminin (22). As shown by ELISA, natural antibodies to these target antigens remained intact after depletion of nonGal xenoantibodies by anti-idiotypic antibody treatment (Figure 7).

A Small Molecule Can Further Reduce Xenoantibody Binding to GTKO endothelial cells after Induction Therapy

Small molecules were screened *in silico* for interaction with the binding pocket of anti-nonGal specific xenoantibody (14). For each of 1,404 compounds included in the NCI Diversity Set III the top 10 binding orientations, or docking poses, were calculated using Autodock vina (18) in combination with PyRx (19). Compounds to be screened *in vitro* were selected by three sequential criteria. First, the top 3,000 of 14,040 total docked poses were selected based on RMSD and affinity. Second, those molecules with less than nine binding orientations included in the top 3,000 were excluded. Those remaining compounds which had at least seven poses with a predicted affinity better than -7.4 kcal/mol were chosen. These criteria were designed to increase the likelihood that compounds selected would have multiple high affinity binding orientations.

Twenty-six compounds (30 μg/ml) were screened *in vitro*, for their ability to inhibit induced anti-nonGal IgM xenoantibody binding by ELISA. Six compounds inhibited over 30% of total binding when using a control induced serum sample from a monkey that had been immunized with 60×10^6 GTKO cells in the absence of treatment with anti-idiotypic antibody (Figure 8). One compound, JMS022, was able to inhibit up to 42% of IgM binding to GTKO endothelial cells. Figure 9a depicts this compound in a predicted high affinity binding orientation with respect to a model of the recombinant anti-nonGal xenoantibody H66K12. JMS022 was then tested further and in triplicate to determine the extent to which it could reduce IgM xenoantibody post immunization from experimental animals. It was able to inhibit 27 ± 4% and 68 ± 9% of the residual GTKO IgM xenoantibody response of Mo-E.B and Mo-E.C respectively. Figure 9b-c illustrates the remaining IgM xenoantibody response after treatment of each animal with both B4N190 *in vivo* and JMS022 *in vitro*. Only Mo-E.B still displayed significant binding above pre-immunization levels.

This suggests that combination treatment utilizing anti-idiotypic antibodies and rationally selected inhibitory small molecules can provide more effective reduction of anti-nonGal xenoantibody responses than treatment with anti-idiotypic antibodies alone. Neither treatment by itself in our experience, to date, was as effective as the combined approach.

Discussion

In this preliminary study, we identify a set of reagents with the ability to specifically target and reduce anti-nonGal xenoantibodies while retaining intact B cell responses to other antigens. Single chain anti-idiotypic mAb pre-treatment *in vivo* prior to xenoantigen exposure combined with small molecule based treatment *in vitro*, as shown here, is capable of inhibiting post-xenotransplant nonGal reactive immunoglobulin in rhesus monkeys exposed to GTKO porcine endothelial cells.

The anti-nonGal IgM xenoantibody response is mediated by a small and structurally similar group of antibodies that pre-exist at low levels but are rapidly induced after xenograft exposure, as shown in our prior studies (13, 14). The use of molecular biology to generate, clone, sequence, and optimize the affinity of novel single chain antibody reagents capable of mitigating this reaction is an approach that has the potential to be advanced into clinical use. Furthermore, extending this work with computer-based structural modeling and small molecule screening provides valuable alternative reagents which provide additional benefit. We have attempted, here, to apply these technologies to address the need for novel and effective methods by which induction of xenoantibodies can be blocked.

Intravenous application of anti-CD20 is currently the most commonly utilized clinically relevant method to mitigate the anti-nonGal xenoantibody response. However, this therapy depletes all $CD20^+$ B cells including naïve, mature, and memory cells (23). Plasma cells are also depleted by extension. While this has been demonstrated to significantly enhance xenograft survival (11), we have demonstrated that it is possible to selectively target B cells mediating xenograft responses. Successful induction using anti-nonGal specific anti-idiotypic antibody can abrogate the xenoantibody response while reducing, but not eliminating, select B cell subsets. Importantly, treatment impacts the differentiation of new plasma cells. Thus both primary and secondary B cell responses should remain relatively intact. Although there is controversy as to their source in humans and nonhuman primates (24, 25), natural antibodies are thought to contribute significantly to immune surveillance (26), normal physiologic processes (27), as well as immune pathologies (28). We demonstrate that several types of natural antibodies remain within normal levels after pretreatment with B4N190.

Anti-idiotypic antibodies have previously been used to modulate humoral immunity in xenotransplantation utilizing two distinct approaches. Polyclonal anti-idiotypic antibody specific for anti-Gal antibody was administered in the form of a vaccination (29, 30). The result was to elicit an anti-anti-idiotypic response composed primarily of IgG_1. These antibodies were meant to replace natural anti-Gal xenoantibody and only marginally activated complement. This approach was shown to significantly prolong the survival of intravenously administered porcine hematopoietic cells. However, anti-idiotypic antibodies

in this study were directed at anti-Gal antibodies. Specifically isolating sufficient quantities of these antibodies from animals provides unique technical challenges limited by the variety of possible nonGal antigens. Thus, we sought alternative methods utilizing antibody sequence analysis.

Schussler et al. attempted direct inhibition of preexisting xenoantibodies using intravenous Ig in a guinea pig to rat model (31). The decreased xenoantibody titer was found to have a strong correlation with graft survival. In this model, however, divalent intravenous Ig was only administered immediately before xenotransplantation. The use of a monovalent preparation weeks before transplant should inhibit anti-nonGal reactive B cells more effectively. Furthermore, use of a monoclonal preparation allows a greater degree of modification to increase efficacy. Thus we used monovalent anti-idiotypic mAb as inductive therapy, with repeated administration several weeks before transplant, and demonstrate diminished xenoantibody responsiveness.

Our previous work, cloning and sequencing immunoglobulin germline gene usage before and after xenotransplantation, revealed increased post-transplant usage of the IgHV3-66 and IgKV1D-12 antibody germline gene progenitors in baboons with active anti-nonGal xenoantibody responses against GTKO/hCD55/hCD59/hHT porcine neonatal islet cell clusters (14). Furthermore, we noted that IgHV3-66 is 86.7% similar to the heavy chain gene IgHV3-21 which encodes the anti-nonGal xenoantibody response of rhesus monkeys against GTKO porcine endothelial cells (13). This high degree of similarity between antibodies elicited in each GTKO xenotransplantation model suggested the feasibility of identifying novel reagents capable of selectively inhibiting induced xenotransplant rejecting anti-nonGal xenoantibodies.

The Griffin.1 phagemid library was specifically chosen to generate anti-idiotypic antibodies because it consists of human derived synthetic scFv ensuring that the resulting mAb would be minimally immunogenic (17). In addition, scFv are monovalent allowing anti-idiotypic scFv to fully inhibit B cell receptor (membrane bound IgM) crosslinking and subsequent activation (32, 33). In contrast, bivalent antibody variable fragments can antagonize activation by polyvalent immunogens but also induce a low level of B cell activation not associated with monovalent scFv. Furthermore, the Griffin.1 library utilizes the pHEN2 vector which can be used to express antibody as scFv alone or attached to filamentous phage during enrichment depending on whether the transformed strain of E. coli is capable of suppressing the amber stop codon.

We have noted a striking similarity in xenoantibody sequences induced in primates in our experience to date (4, 13-15, 34). The similarity of anti-nonGal idiotypes across species is further emphasized by the relatively high efficacy noted in rhesus monkeys using a combination of reagents that were generated by targeting a xenoantibody structure identified in baboons. The methods by which these reagents were generated can easily be adjusted to better suit the subtle differences of the human immune response, if necessary.

The inhibitory small molecules identified with virtual screening in this study will be important to test for efficacy *in vivo*, but prior investigation of metabolism and toxicology

will be necessary before use in large animal models. Screening small molecule libraries which already have FDA approval, such as the NIH clinical collection, should expedite our progress in large animal experiments using compounds newly identified *in silico*. Although molecular inhibitors of the anti-Gal antibodies could be developed rationally based on α 1,3 gal structure (1) the identity of the nonGal xenoantigen(s) is currently highly debated (35-37). Over the past decade, computational approaches to drug discovery have been gaining traction (38). The combination of homology modeling and structure-based *in silico* screening for bioactive small molecules has been successfully used to aid more traditional pharmacologic screening techniques (38-40). However, the application of this technology to develop inhibitors of antibodies has been restricted by the limited number of deposited antibody crystal structures and the complexities of modeling poorly conserved complementary determining regions; both limitations which are steadily being overcome (41, 42). We successfully applied this technology, in combination with our previous analysis of the anti-nonGal xenoantibody response (13, 14), to rationally search for small molecules capable of inhibiting anti-nonGal xenoantibody. Although further optimization is required, our initial results are promising.

Anti-idiotypic antibodies and small molecules with specificity for anti-nonGal antibodies, to our knowledge, have not been reported by others. The application of these reagents to inhibit xenoantibody responses to GTKO xenografts is feasible due to the fact that anti-nonGal antibodies naturally exist at low levels (43). Thus smaller amounts of anti-nonGal specific reagents would be required before transplant to directly inhibit preexisting xenoantibodies, preempting the formation of a strong anti-nonGal adaptive immune response. In this report we provide data documenting feasibility, although further optimization of the induction regimen will be required.

Given the limited impact of anti-id treatment on the IgM response, further studies should focus on refining this approach to generate a more broadly efficacious treatment. However, the currently achievable impact on the IgG response suggests pretreatment with B4N190 may be beneficial in select xenotransplantation models. For example, success of engraftment in mixed chimerism has been found to be inversely correlated with the level of anti-nonGal IgG in the recipient animal (44). Therefore, B4N190 may enhance the level of GTKO pig-to-primate bone marrow chimerism which can be achieved. The application of these reagents in pig-to-primate models of islet as well as solid organ xenotransplantation will require further optimization. At present, the combination of these reagents was only able to impact the IgM xenoantibody response of two out of three experimental animals. This suggests that there is some degree of anti-nonGal xenoantibody structural variation between animals. We speculate that previously noted differences in the xenoantibody CDR3 sequences (14) may sufficiently alter the anti-nonGal idiotype so as to interfere with the efficacy of these reagents. Variations in the CDR3, which are at the center of the antigen binding pocket, could alter the relative positions of the heavy and light chains. This inherent variation can be addressed by using methods which target idiotypic regions with less structural variability. Once these initial obstacles are overcome it will be possible to determine how best to combine reagents which target anti-nonGal xenoantibody with current immunosuppressive protocols.

Acknowledgments

GTKO endothelial cells (PEGKO42) were kindly provided by Dr. David Sachs, Massachusetts General Hospital. We also thank Hector Almanzar, Billy Watson, and Michele Martinez for technical assistance. This work was supported by NIH grant #RO1AI052079 (MKJ) and the Primate Center base operating grant #OD011107 (AFT).

Abbreviations

nonGal	non α-1,3-gal
GTKO	α-1,3-galactosyltransferase knockout
DHXR	delayed humoral xenograft rejection
mAb	monoclonal antibody
scFv	single chain variable fragment
ssDNA	single stranded DNA
SEM	standard error of the mean
i.v.	intravenous

References

1. Katopodis AG, Warner RG, Duthaler RO, et al. Removal of anti-Galalpha1,3Gal xenoantibodies with an injectable polymer. J Clin Invest. 2002; 110:1869–1877. [PubMed: 12488437]
2. Lai L, Kolber-Simonds D, Park KW, et al. Production of α-1, 3-galactosyltransferase knockout pigs by nuclear transfer cloning. Science. 2002; 295:1089–1092. [PubMed: 11778012]
3. Phelps CJ, Koike C, Vaught TD, et al. Production of alpha 1,3-galactosyltransferase-deficient pigs. Science. 2003; 299:411–414. [PubMed: 12493821]
4. Fischer-Lougheed JY, Tarantal AF, Shulkin I, et al. Gene therapy to inhibit xenoantibody production using lentiviral vectors in non-human primates. Gene Ther. 2007; 14:49–57. [PubMed: 16886002]
5. Rieben R, Bovin NV, Korchagina EY, et al. Xenotransplantation: in vitro analysis of synthetic α-galactosyl inhibitors of human anti-Galα1→ 3Gal IgM and IgG antibodies. Glycobiology. 2000; 10:141–148. [PubMed: 10642605]
6. Ekser B, Klein E, He J, et al. Genetically-engineered pig-to-baboon liver xenotransplantation: histopathology of xenografts and native organs. PloS one. 2012; 7:e29720. [PubMed: 22247784]
7. Shimizu A, Yamada K, Robson SC, Sachs DH, Colvin RB. Pathologic characteristics of transplanted kidney xenografts. J Am Soc Nephrol: JASN. 2012; 23:225–235.
8. Le Bas-Bernardet S, Tillou X, Poirier N, et al. Xenotransplantation of Galactosyl-Transferase Knockout, CD55, CD59, CD39, and Fucosyl-Transferase Transgenic Pig Kidneys Into Baboons. Transplant Proc. 2011; 43:3426–3430. [PubMed: 22099813]
9. Tazelaar HD, Byrne GW, Mcgregor CGA. Comparison of Gal and Non-Gal-Mediated Cardiac Xenograft Rejection. Transplantation. 2011; 91:968–975. [PubMed: 21403591]
10. Mcgregor CGA, Ricci D, Miyagi N, et al. Human CD55 Expression Blocks Hyperacute Rejection and Restricts Complement Activation in Gal Knockout Cardiac Xenografts. Transplantation. 2012; 93:686–692. [PubMed: 22391577]
11. Mohiuddin MM, Corcoran PC, Singh AK, et al. B-Cell Depletion Extends the Survival of GTKO.hCD46Tg Pig Heart Xenografts in Baboons for up to 8 Months. Am J Transplant. 2012; 12:763–771. [PubMed: 22070772]
12. Kamar N, Milioto O, Puissant-Lubrano B, et al. Incidence and Predictive Factors for Infectious Disease after Rituximab Therapy in Kidney-Transplant Patients. Am J Transplant. 2010; 10:89–98. [PubMed: 19656128]

13. Kiernan K, Harnden I, Gunthart M, et al. The anti-non-gal xenoantibody response to xenoantigens on gal knockout pig cells is encoded by a restricted number of germline progenitors. Am J Transplant. 2008; 8:1829–1839. [PubMed: 18671678]
14. Chen Y, Stewart JM, Gunthart M, et al. Xenoantibody Response to Porcine Islet Cell Transplantation using GTKO, CD55, CD59, and Fucosyl-Transferase Multiple Transgenic Donors. Xenotransplantation. 2014 In Press.
15. Kearns-Jonker M, Swensson J, Ghiuzeli C, et al. The human antibody response to porcine xenoantigens is encoded by IGHV3-11 and IGHV3-74 IgVH germline progenitors. J Immunol. 1999; 163:4399–4412. [PubMed: 10510381]
16. Rasband, WS. ImageJ Bethesda. Maryland, USA: U.S. NIH; p. 1997-2012.
17. Griffiths AD, Williams SC, Hartley O, et al. Isolation of high-affinity human-antibodies directly from large synthetic repertoires. Embo J. 1994; 13:3245–3260. [PubMed: 8045255]
18. Trott O, Olson AJ. AutoDock Vina: improving the speed and accuracy of docking with a new scoring function, efficient optimization, and multithreading. J Comput Chem. 2010; 31:455–461. [PubMed: 19499576]
19. Wolf LK. New software and Websites for the Chemical Enterprise. Chem Eng News. 2009; 31
20. Kearns-Jonker M, Fischer-Lougheed J, Shulkin I, et al. Use of lentiviral vectors to induce long-term tolerance to gal(+) heart grafts. Transplantation. 2004; 77:1748–1754. [PubMed: 15201677]
21. De Bruin R, Spelt K, Mol J, Koes R, Quattrocchio F. Selection of high-affinity phage antibodies from phage display libraries. Nat biotechnology. 1999; 17:397–399.
22. Dimitrijevic LA, Stojanovic M, Ciric B, et al. Expression of Y7 cross-reactive idiotope on human IgM molecules. Immunol Invest. 2004; 33:1–14. [PubMed: 15015828]
23. Leandro MJ. B-cell subpopulations in humans and their differential susceptibility to depletion with anti-CD20 monoclonal antibodies. Arthritis Res Ther. 2013; 15(Suppl 1):S3. [PubMed: 23566754]
24. Griffin DO, Holodick NE, Rothstein TL. Human B1 cells in umbilical cord and adult peripheral blood express the novel phenotype CD20+ CD27+ CD43+ CD70. Journal Exp Med. 2011; 208:67–80. [PubMed: 21220451]
25. Covens K, Verbinnen B, Geukens N, et al. Characterization of proposed human B-1 cells reveals pre-plasmablast phenotype. Blood. 2013; 121:5176–5183. [PubMed: 23613519]
26. Baumgarth N, Herman OC, Jager GC, et al. B-1 and B-2 cell-derived immunoglobulin M antibodies are nonredundant components of the protective response to influenza virus infection. J Exp Med. 2000; 192:271–280. [PubMed: 10899913]
27. Baumgarth N. The double life of a B-1 cell: self-reactivity selects for protective effector functions. Nat Rev Immunol. 2011; 11:34–46. [PubMed: 21151033]
28. Boes M, Schmidt T, Linkemann K, et al. Accelerated development of IgG autoantibodies and autoimmune disease in the absence of secreted IgM. Proc Nat Acad Sci USA. 2000; 97:1184–1189. [PubMed: 10655505]
29. Hernandez AM, Rodriguez N, Gonzalez JE, et al. Anti-NeuGcGM3 Antibodies, Actively Elicited by Idiotypic Vaccination in Nonsmall Cell Lung Cancer Patients, Induce Tumor Cell Death by an Oncosis-Like Mechanism. J Immunol. 2011; 186:3735–3744. [PubMed: 21300821]
30. Mcmorrow IM, Buhler L, Treter S, et al. Modulation of the in vivo primate anti-Gal response through administration of anti-idiotypic antibodies. Xenotransplantation. 2002; 9:106–114. [PubMed: 11897003]
31. Schussler O, Genevaz D, Latremouille C, et al. Intravenous immunoglobulins for therapeutic use contain anti-idiotypes against xenophile antibodies and prolong discordant graft survival. Clin Immunol Immunopathol. 1998; 86:183–191. [PubMed: 9473381]
32. Minguet S, Dopfer EP, Schamel WWA. Low-valency, but not monovalent, antigens trigger the B-cell antigen receptor (BCR). Int Immunol. 2010; 22:205–212. [PubMed: 20145007]
33. Kim YM, Pan JYJ, Korbel GA, et al. Monovalent ligation of the B cell receptor induces receptor activation but fails to promote antigen presentation. Proc Nat Acad Sci USA. 2006; 103:3327–3332. [PubMed: 16492756]
34. Baquerizo A, Mhoyan A, Kearns-Jonker M, et al. Characterization of human xenoreactive antibodies in liver failure patients exposed to pig hepatocytes after bioartificial liver treatment: an

ex vivo model of pig to human xenotransplantation. Transplantation. 1999; 67:5–18. [PubMed: 9921790]

35. Chihara RK, Lutz AJ, Paris LL, et al. Fibronectin from alpha 1,3-galactosyltransferase knockout pigs is a xenoantigen. J Surg Res. 2013
36. Breimer ME. Gal/non-Gal antigens in pig tissues and human non-Gal antibodies in the GalT-KO era. Xenotransplantation. 2011; 18:215–228. [PubMed: 21848538]
37. Byrne GW, Stalboerger PG, Davila E, et al. Proteomic identification of non-Gal antibody targets after pig-to-primate cardiac xenotransplantation. Xenotransplantation. 2008; 15:268–276. [PubMed: 18957049]
38. Ekins S, Mestres J, Testa B. In silico pharmacology for drug discovery: methods for virtual ligand screening and profiling. Br J Pharmacol. 2007; 152:9–20. [PubMed: 17549047]
39. Evers A, Klebe G. Successful virtual screening for a submicromolar antagonist of the neurokinin-1 receptor based on a ligand-supported homology model. J Med Chem. 2004; 47:5381–5392. [PubMed: 15481976]
40. Evers A, Klabunde T. Structure-based drug discovery using GPCR homology modeling: Successful virtual screening for antagonists of the Alpha1A adrenergic receptor. J Med Chem. 2005; 48:1088–1097. [PubMed: 15715476]
41. Kuroda D, Shirai H, Jacobson MP, Nakamura H. Computer-aided antibody design. Protein Eng Des Sel: PEDS. 2012; 25:507–521.
42. Sivasubramanian A, Sircar A, Chaudhury S, Gray JJ. Toward high-resolution homology modeling of antibody Fv regions and application to antibody-antigen docking. Proteins. 2009; 74:497–514. [PubMed: 19062174]
43. Harnden I, Kiernan K, Kearns-Jonker M. The anti-nonGal xenoantibody response to alpha1,3-galactosyltransferase gene knockout pig xenografts. Curr Opin Organ Transplant. 2010; 15:207–211. [PubMed: 20075731]
44. Liang F, Wamala I, Scalea J, et al. Increased levels of anti-non-Gal IgG following pig-to-baboon bone marrow transplantation correlate with failure of engraftment. Xenotransplantation. 2013; 20:458–468. [PubMed: 24289469]

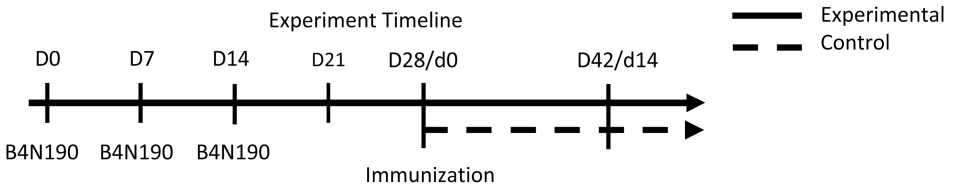

Figure 1. ***In vivo*** **Experimental time line**

Five juvenile (11-12 months; 2.1-2.4 kg) rhesus monkeys were selected for low preexisting levels of anti-nonGal IgM xenoantibody. An anti-nonGal xenoantibody response was initiated in two control animals (Mo-C.A and Mo-C.B) by intravenous injection with 60×10^6 GTKO porcine endothelial cells. Three experimental monkeys were pretreated with once weekly intravenous injections of the anti-nonGal specific anti-idiotypic antibody, B4N190, for three weeks. At experimental day 28 experimental animals Mo-E.A, Mo-E.B, and Mo-E.C were intravenously injected with 60×10^6, 15×10^6, 7.5×10^6 GTKO porcine endothelial cells respectively. Serum was collected at each experimental time point. Experimental Day number (**D**); day post immunization (**d**).

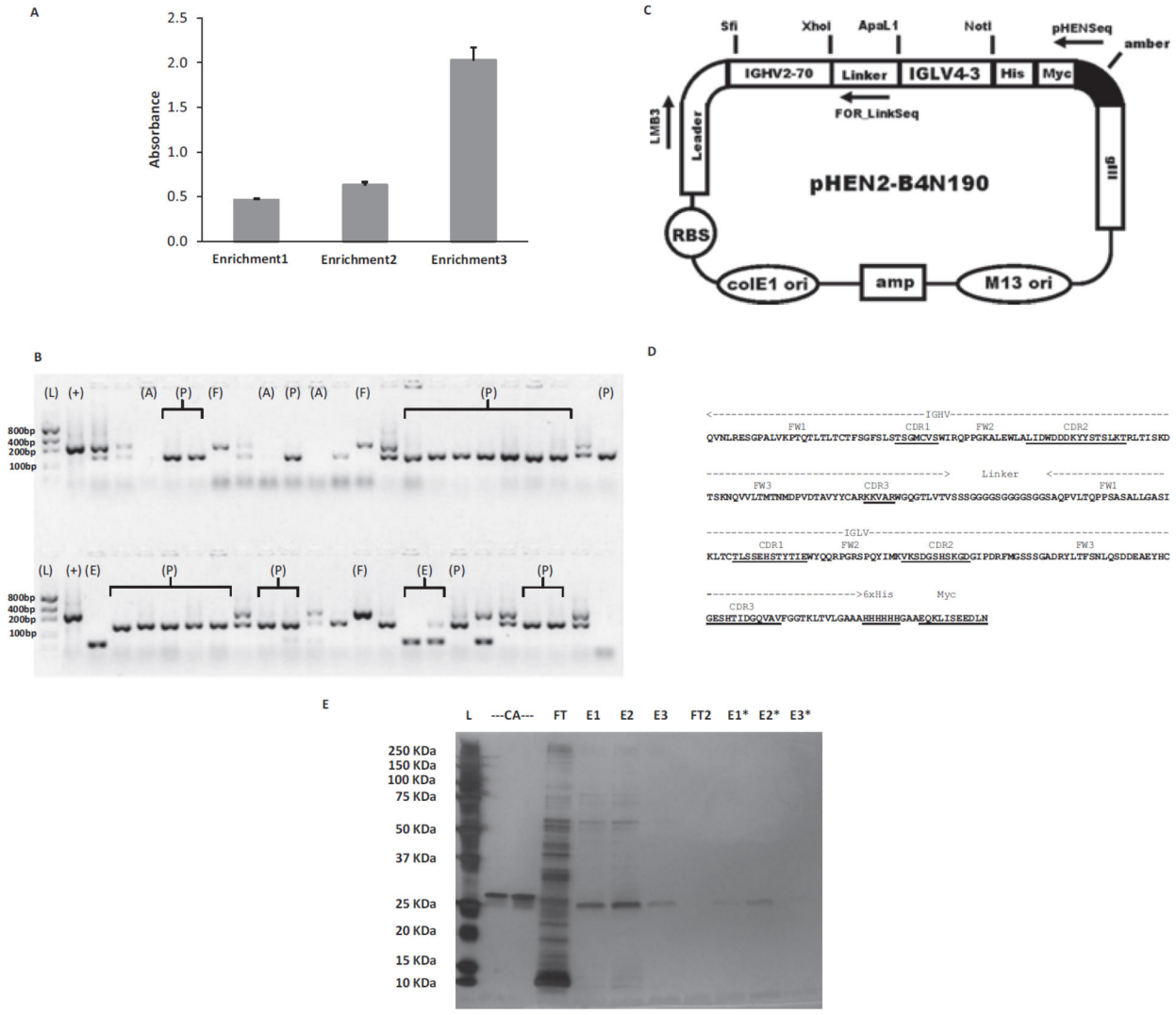

Figure 2. Generation of single chain anti-idiotypic antibody with specificity for anti-nonGal xenoantibody

A human-derived synthetic antibody phage display library was used to generate anti-nonGal xenoantibody specific anti-idiotypic antibody. **(A)** Increased total binding of polyclonal anti-nonGal-reactive phage to purified H66K12 after each round of enrichment by ELISA. Values are reported as mean absorbance ± SEM. **(B)** nonGal-reactive pHEN2 DNA was screened for full length inserts by polymerase chain reaction and gel electrophoresis. A typical screen included less than 10% full length single chain constructs. In contrast, the majority of constructs contained partial inserts, including either a light or heavy chain variable region but not both. **(C)** Schematic of pHEN2 phagemid encoding single chain antibody B4N190 encoded by the IGHV2-70 and IGLV4-3 antibody germline genes. **(D)** Amino acid translation of B4N190 the recombinant single chain anti-nonGal xenoantibody specific anti-idiotypic antibody. **(E)** B4N190 was purified using a combination of ammonium sulfate precipitation and nickel column chromatography. A representative SDS-PAGE silver stained for total protein representing the final product used for *in vivo* experimentation. B4N190 was purified a second time as required to ensure purity.

Prestained ladder allows visual determination of gel resolution before silver staining but by necessity is over exposed in the final image. Immunoglobulin heavy chain variable region (**IGHV**); frame work region (**FW**); complementary determining region (**CDR**); immunoglobulin light chain variable region (**IGLV**); ladder (**L**); positive control (+); absent construct (**A**); empty construct (**E**); partial construct (**P**); full length construct (**F**); carbonic anhydrase (**CA**); flow through (**FT**); elution 1st purification (**E**); elution 2nd purification (**E***);

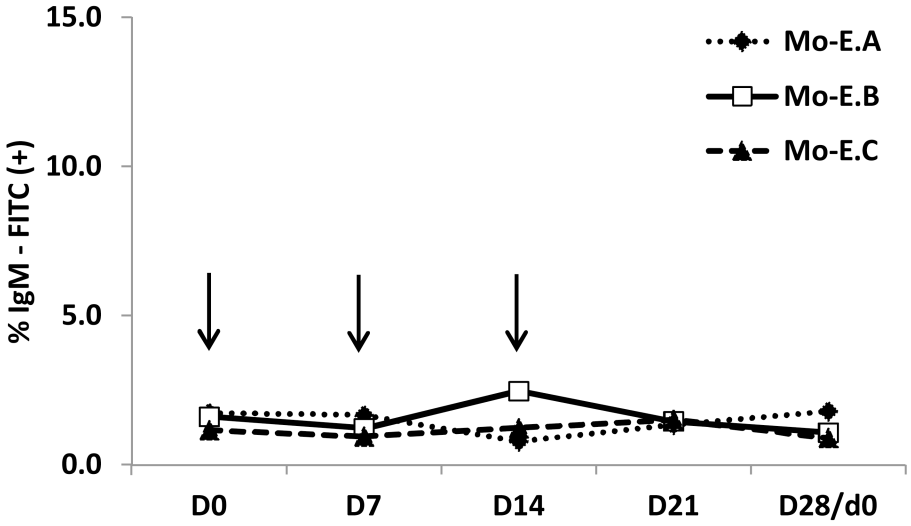

Figure 3. Induction therapy with B4N190 does not alter preexisting, low anti-nonGal IgM xenoantibody levels

Anti-nonGal IgM xenoantibody was monitored weekly by flow cytometry against GTKO porcine endothelial cells. Three experimental animals (**Mo-E.A**, **Mo-E.B**, **Mo-E.C**) were treated with the anti-nonGal specific anti-idiotypic antibody B4N190 on experimental day 0, 7, and 14 (**arrow**). However, the anti-nonGal IgM xenoantibody level remains constant (0.9-2.5% positive staining).

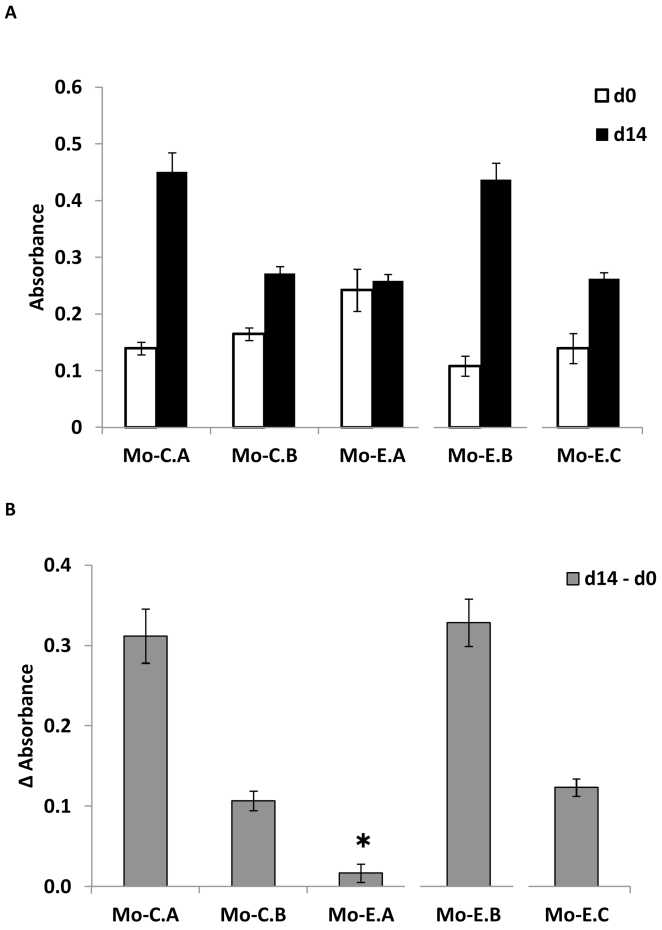

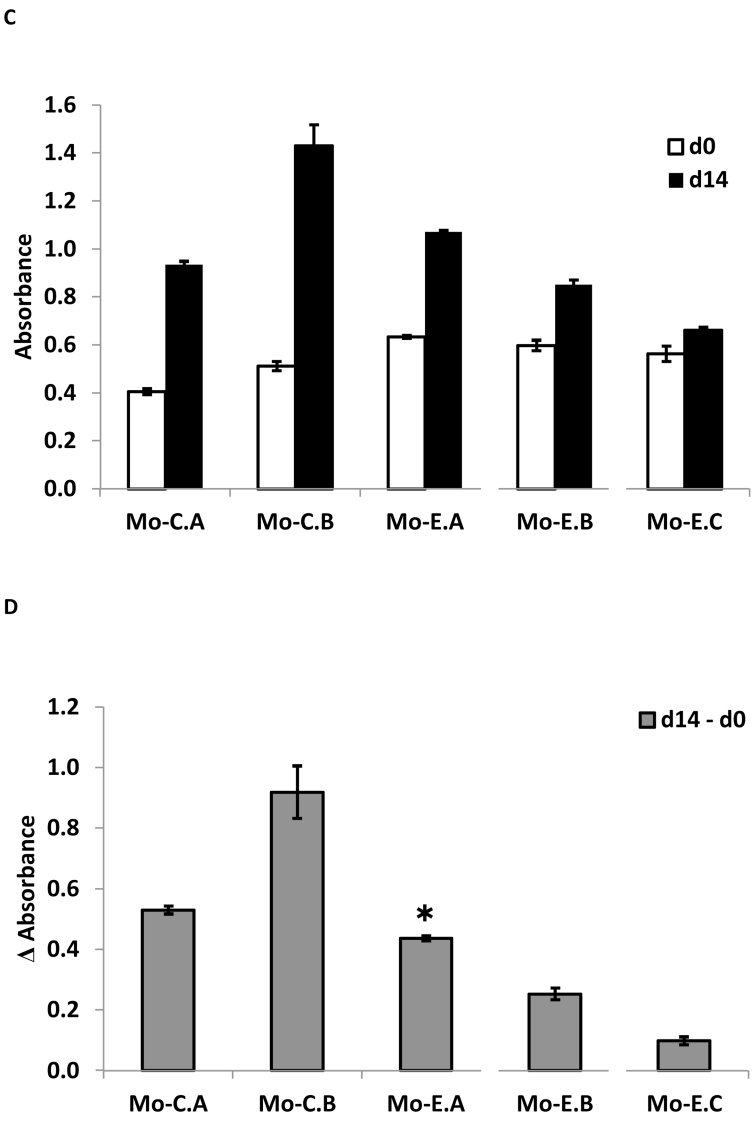

Figure 4. Induction therapy with B4N190 significantly reduces the induced xenoantibody response

Anti-nonGal IgM **(A and B)** and IgG **(C and D)** xenoantibody of both control (**Mo-C.A** and **Mo-C.B**) and experimental animals (**Mo-E.A**, **Mo-E.B**, **Mo-E.C**) were measured by ELISA at day 0 and 14 after immunization with GTKO porcine endothelial cells. Mo-C.A, Mo-C.B, and Mo-E.A were immunized with 60×10^6 cells and are thus are directly comparable. Mo-E.B and Mo-E.C were immunized with 15 and 7.5×10^6 cells respectively. Data is represented as total xenoantibody **(A and C)** and the xenoantibody response (d14-d0) **(B and D)**. Mo-E.A demonstrates a reduced IgM xenoantibody response compared to matched control animals. All experimental animals displayed reduced IgG xenoantibody responses compared to controls. Values are reported as mean absorbance or Δ absorbance ± SEM of four technical replicates; ***** indicates a significant difference ($p < 0.05$) compared to Mo-C.A as well as Mo-C.B; day post immunization (**d**).

A

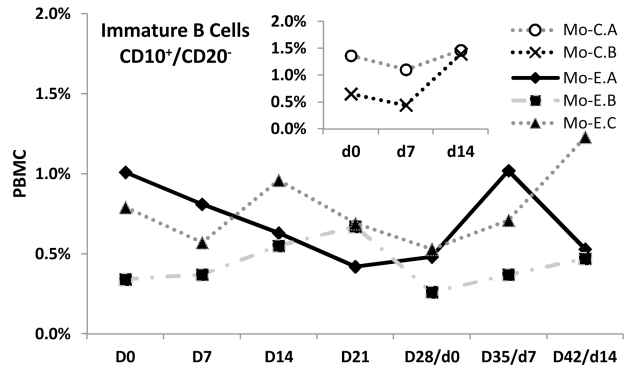

B

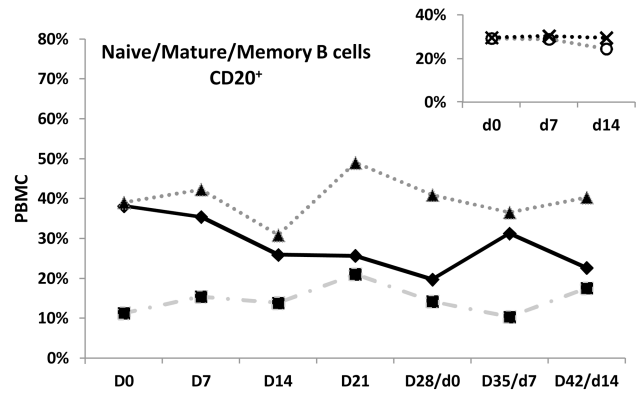

C

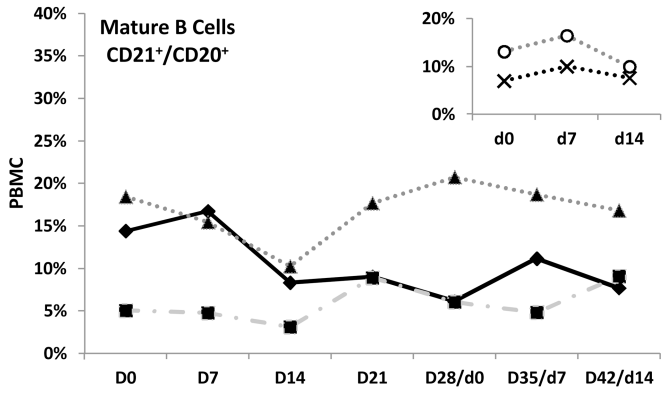

D

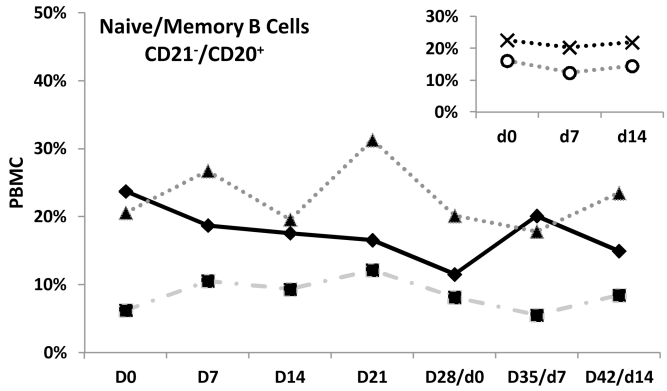

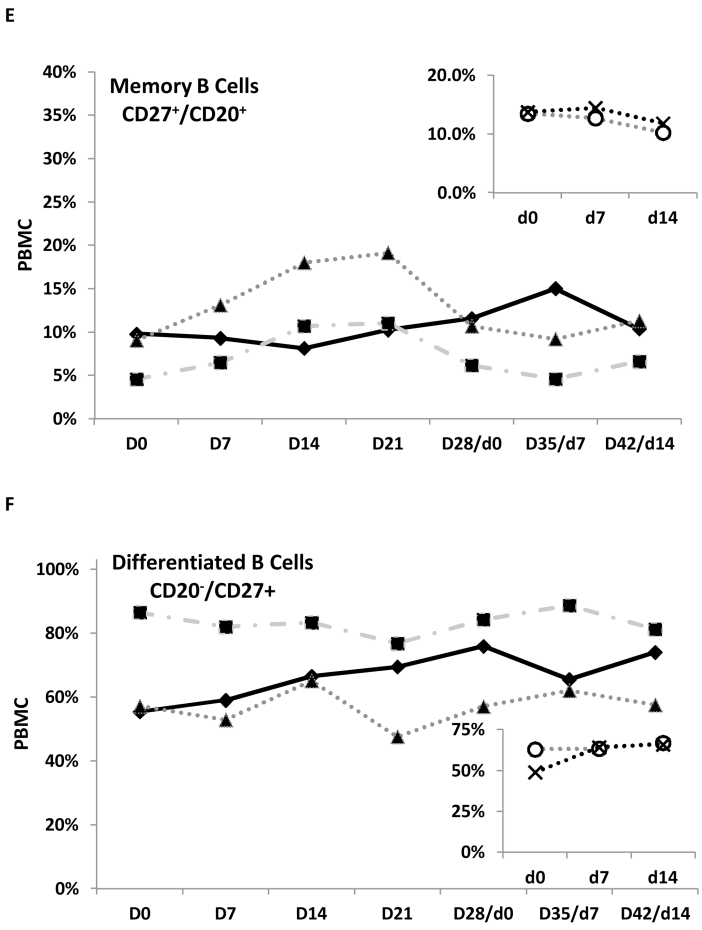

Figure 5. Induction therapy with B4N190 reduces, but does not deplete, select B cell subsets

Specific B cell subsets of both control (inset) and experimental animals were monitored by flow cytometry over the course of the experiment including: **(A)** immature B cells ($CD10^+$/$CD20^-$), **(B)** total $CD20^+$ B cells (naïve/mature/memory), **(C)** mature B cells ($CD20^+$/$CD21^+$), **(D)** $CD20^+$/$CD21^-$ B cells (naïve/memory), **(E)** memory B cells ($CD20^+$/$CD27^+$), and **(F)** differentiated B cells ($CD20^-$/$CD27^+$). A reduction of several subsets was associated with the reduction of the anti-nonGal IgM and IgG xenoantibody responses of Mo-E.A. Those subsets reduced included immature, total $CD20^+$, naïve, and mature B cells, but not memory or differentiated B cells. Control animals **Mo-C.A** and **Mo-C.B**; Experimental animals **Mo-E.A**, **Mo-E.B**, and **Mo-E.C**

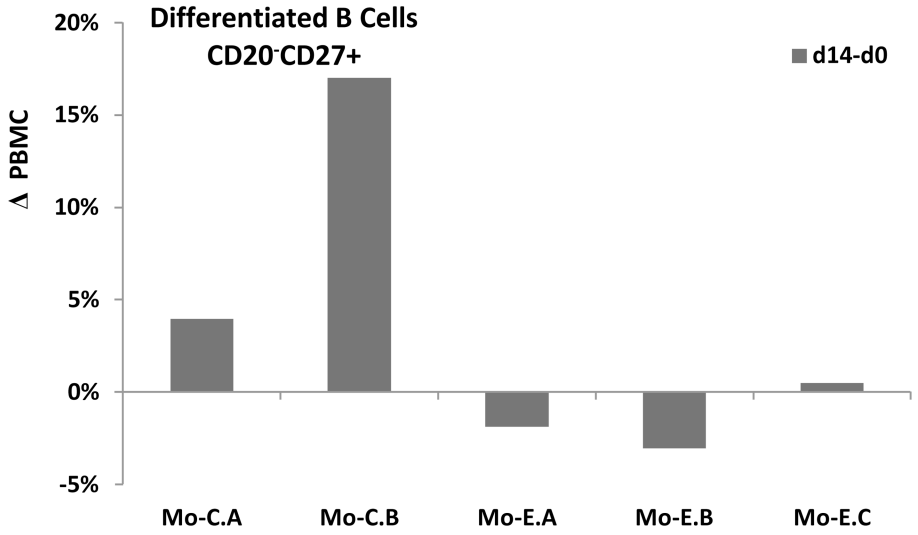

Figure 6. Induction therapy is associated with reduced differentiated B cell formation after xenotransplantation

Differentiated B cell ($CD20^-/CD27^+$) count was monitored over the course of the study. After immunization with GTKO porcine endothelial cells analysis revealed that control animals displayed an increase in differentiated B cell count while animals treated with B4N190 demonstrated no change or a reduction in differentiated B cell count. Control animals **Mo-C.A** and **Mo-C.B**; Experimental animals **Mo-E.A**, **Mo-E.B**, and **Mo-E.C**

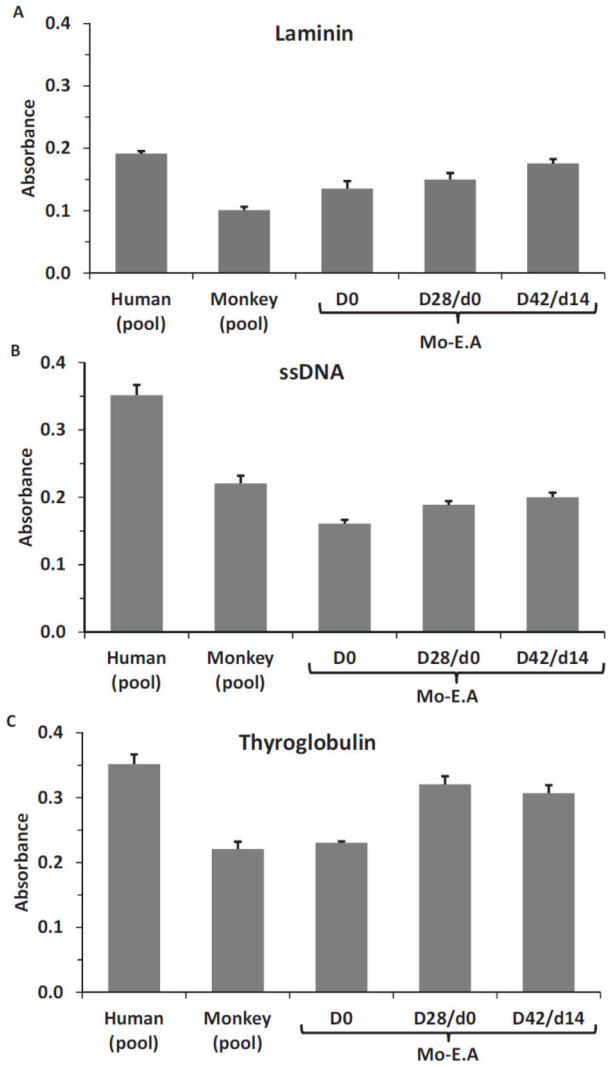

Figure 7. Natural antibodies are not affected by induction therapy with B4N190

Because Mo-E.A is the only animal that displayed a reduction of both the anti-nonGal IgM and IgG xenoantibody responses we sought to determine if other antibody responses of this animal were still left intact. Serum was tested to determine if natural antibodies capable of binding **(A)** laminin, **(B)** ssDNA, and **(C)** thyroglobulin were affected by B4N190. Pooled monkey and pooled human serum were used to assess the normal range of natural antibodies. Induction therapy of Mo-E.A which was associated with reduced anti-nonGal IgM and IgG xenoantibody responses did not affect any of these natural antibodies. Values are reported as mean absorbance ± SEM. Experimental Day (**D**); day after immunization (**d**)

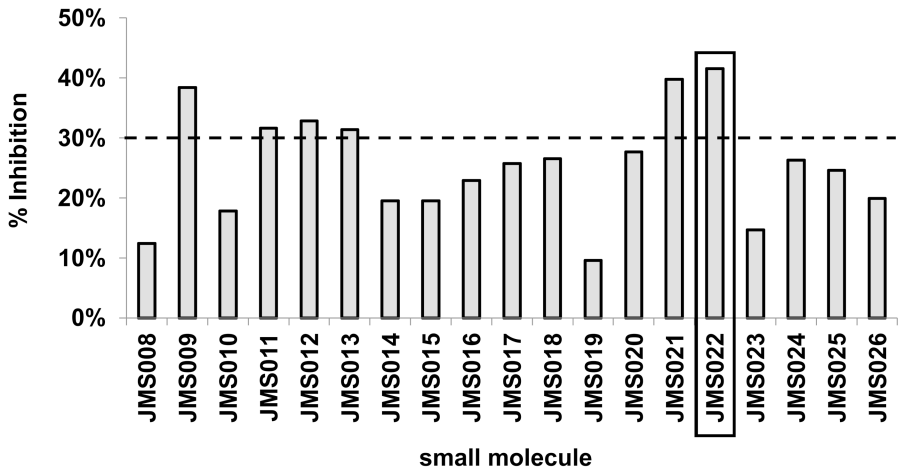

Figure 8. Virtual screening is an efficient identifier of small molecules capable of inhibiting anti-nonGal IgM xenoantibody

The ability of small molecules to inhibit anti-nonGal IgM xenoantibody was measured by ELISA against GTKO porcine endothelial cells. Initial *in vitro* screening demonstrated the efficiency with which virtual screening is capable of identifying potent inhibitory small molecules. Six out of 19 molecules (30 uM) from a representative experiment were capable of inhibiting at least 30% of total d14 post immunization anti-nonGal IgM in serum (1:30) from Mo-C.A. On further evaluation, JMS022 (box) was capable of inhibiting a greater percentage of induced IgM xenoantibody from other post-transplant samples (see Figure 9).

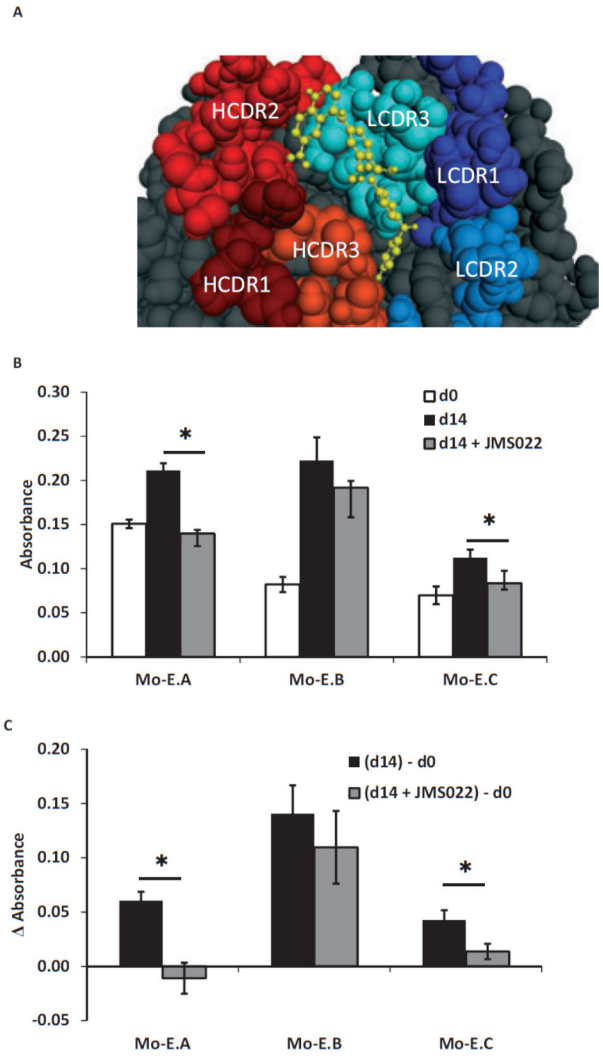

Figure 9. A small molecule inhibitor, JMS022, in addition to B4N190 provides more effective treatment

When tested at 14 days post immunization of experimental animals, a small molecule JMS022, was able to inhibit 27 ± 4% and 68 ± 9% of the IgM xenoantibody response of Mo-E.B and Mo-E.C, respectively. **(A)** This 521 Da benzamide, JMS022 (yellow), is depicted binding to H66K12 in a representative high affinity binding mode predicted *in silico*. **(B-C)** After treatment with both B4N190 *in vivo* and JMS022 *in vitro* only Mo-E.B still displayed significant IgM binding above pre-immunization levels. Values are reported as mean absorbance ± SEM. Heavy chain complementary determining region (**HCDR**); light chain complementary determining region (**LCDR**); day 0 immunization (**d0**); day 14 immunization (**d14**); Experimental animals **Mo-E.A**, **Mo-E.B**, and **Mo-E.C**

Table 1

Absolute number of PBMC analyzed at each experimental time point

	D0	D7	D14	D21	D28/d0	D35/d7	D42/d14
Mo-E.A	1.9×10^6	3.5×10^6	3.5×10^6	5.8×10^6	4.1×10^6	4.3×10^6	4.9×10^6
Mo-E.B	4.1×10^6	3.6×10^6	2.5×10^6	3.0×10^6	5.5×10^6	5.3×10^6	1.8×10^6
Mo-E.C	6.1×10^6	4.5×10^6	4.3×10^6	3.5×10^6	5.8×10^6	7.2×10^6	3.1×10^6
Mo-C.A					5.2×10^6	3.8×10^6	6.0×10^6
Mo-C.B					4.6×10^6	3.3×10^6	7.4×10^6